Jordi Rius*, Oriol Vallcorba, Anna Crespi and Fernando Colombo

Increasing data completeness in synchrotron tts-microdiffraction experiments for δ-recycling phasing of low-symmetry compounds

DOI 10.1515/zkri-2017-2064
Received April 7, 2017; accepted May 30, 2017

Abstract: Successful phasing of synchrotron through-the-substrate microdiffraction data by δ-recycling direct-methods largely depends on the number of missing intensities caused by the limited sample rotation range [J. Rius, Direct phasing from Patterson syntheses by δ recycling. *Acta Cryst. A* **2012**, *68*, 77–81]. Particularly, for the unfavorable triclinic system, dataset completeness resulting from a single series of consecutive ϕ-scans covering a total ϕ interval of ±35° is around 41%. This value is not enough for the routinary solution of a crystal structure by δ-recycling but can be increased by ~29% by applying the orthogonal χ strategy consisting of merging the information of two series of orthogonal ϕ-scans collected at the same microvolume of the polished thin section. Test calculations using simulated and experimental tts-data of the triclinic mineral axinite confirm that, with the help of the orthogonal χ strategy, crystal structures can be solved routinely. Since data in the ±35 ϕ-interval are normally accessible even for relatively thick glass-substrates (1–1.5 mm), a crystal structure can be determined from a single microvolume. For high-symmetry phases, due to the Laue symmetry redundancy, a single series of ϕ-scans normally suffices for the application of δ-recycling. However, when for experimental causes this series is incomplete, the orthogonal χ strategy also provides a simple way to increase the completeness which besides allowing solving the structure, is also beneficial for the subsequent refinement.

***Corresponding author: Jordi Rius,** Institut de Ciència de Materials de Barcelona, CSIC, Campus de la UAB, 08193 Bellaterra, Catalonia, Spain, E-mail: jordi.rius@icmab.es
Oriol Vallcorba: ALBA Synchrotron Light Source, carrer de la Llum 2-26, Cerdanyola del Vallès, Barcelona, Spain
Anna Crespi: Institut de Ciència de Materials de Barcelona, CSIC, Campus de la UAB, 08193 Bellaterra, Catalonia, Spain
Fernando Colombo: CICTERRA-Universidad Nac. Córdoba, CONICET, Vélez Sarsfield 1611, Córdoba, X50166CA, Argentina

Keywords: δ recycling phasing; polished thin sections; structure solution; synchrotron tts-μXRD; X-ray data completeness.

Introduction

Polished thin sections of rocks with the specimen fixed on a glass-substrate are commonly used in mineralogical, petrological and cultural heritage studies. Thin sections with specimen thicknesses up to 30 μm are not only ideal for the microscopic observation but also for determining the optical properties under plane polarized transmitted light. These studies can be complemented with electron microprobe analyses at selected points of the polished section and, also, with SEM-EDS-BSE (SEM, scanning electron microscopy; EDS, energy-dispersive spectroscopy; BSE, backscattered electron) analyses and images. Due to their local character all these techniques can be applied to inhomogeneous samples. When diffraction information of specific regions of the thin section is needed the ideal technique is through-the-substrate transmission microdiffraction, tts-μXRD [1]. Due to the simple experimental setup (Figure 1), measurement in transmission greatly simplifies data reduction. The only negative aspect is the beam attenuation caused by the glass-substrate which can be solved with synchrotron radiation combining high flux and a short wavelength.

In a related paper [2] synchrotron tts-μXRD was applied to crystal structure solution by using data from single series of ϕ-scans taken at multiple microvolumes in the polished thin-section. (Individual ϕ-scans are characterized by their angular increment $\Delta\phi$ [mostly between 5 and 10°] and their offset angle or centre). To increase the measurement speed and to generate less data, a specific scanning mode was introduced. According to it, if the total number of frames in a given series is $2m+1$, then the individual ϕ-scans are centered at $\phi_i = i \cdot \Delta\phi$ with angular limits given by $[(i-1)\cdot\Delta\phi, (i+1)\cdot\Delta\phi]$, $(i = 0, \pm1, \pm2 \ldots \pm m)$. This ensures that each diffraction spot is measured twice, so that a spot lying at the border of one ϕ-scan falls amidst the neighboring ϕ-scan. Due to the partial overlap between

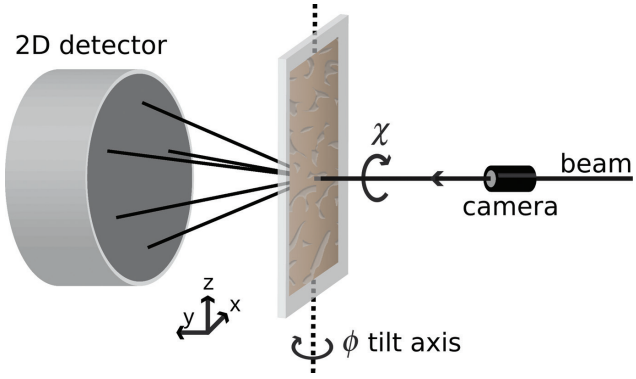

Fig. 1: Setup for microdiffraction on polished thin sections. The target point (microvolume) is searched on the *xz* plane. The diffraction pattern is collected by rotating the thin section around the ϕ axis (dark part = thin-section, light part = glass-substrate). The number of measured intensities can be increased by performing additional ϕ-scans at different χ rotations.

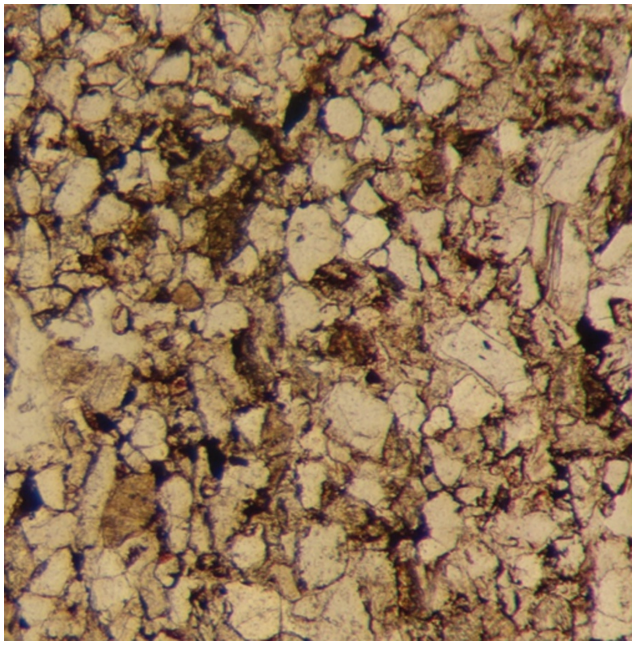

Fig. 2: Photomicrograph (1.5×1.5 mm^2) showing the microstructure of quartz-arenite in the polished thin section (sample thickness ~30 μm).

frames subsequent frame-merging (allowing for diffracting volume variations) is robust and ends with a reliable partial *hkl* dataset. The last step consists of merging the partial *hkl* datasets of all equivalent microvolumes (multicrystal-merging). The quality of frame- and multicrystal-merging is checked with the R_{frame} and R_{mult} residuals given in Rius et al. [2]. Multicrystal-merging is simple for holohedral Laue groups but somewhat more complicated for merohedral compounds. This can be illustrated by measuring five quartz microcrystals located in the polished thin-section of a quartzarenite sample (Figure 2; quartzarenite is a sandstone composed of greater than 90% detrital quartz). Since quartz belongs to the Laue group $\bar{3}m1$, the merging is hemihedral, i.e. the *hkl* choice between the two sets of indices is arbitrarily fixed for the first dataset, but then assignments for the rest of crystal datasets must be consistent with this choice. Of the 16 (=2^{5-1}) possibilities the best combination of *hkl* choices clearly stands out by its lowest R_{mult} value (2.5% compared to 15% for the next ranked one) yielding a merged *hkl* dataset of 84.31% completeness. Since the focus of this paper was primarily on the completion of *hkl* datasets by multicrystal merging, information of single target points was not exhaustively exploited. This is why it was decided to explore a new data collection strategy yielding more intensity data from a single microvolume to help to increase the efficiency of δ-recycling phasing. Needless to say, that optimizing data acquisition from a single microvolume is also beneficial for crystal structure refinement, because the number of required microvolumes is reduced and, consequently, eventual chemical inhomogeneity is minimized.

The efficiency of δ-recycling as a function of completeness will be studied on a triclinic example. For convenience, the two completeness definitions $c_{acc}=N_{acc}/N_{asy}$ and $c_{obs}=N_{obs}/N_{asy}$ will be used. In these expressions N_{acc}, N_{obs} and N_{asy} are, respectively, the number of symmetrically-independent accessible, observed and total number of reflections in the asymmetrical unit of reciprocal space. The triclinic is a representative test case, since there is only the intensity redundancy due to the Laue inversion center.

Generalities of the δ-recycling structure solution method

In the present work structure solution tests are performed by applying the two-stage δ-recycling method [3, 4]. This method is formally close to the charge-flipping method [5, 6] but differs in the way the electron density function is modified and does not involve any flipping operation. In its first stage it minimizes the discrepancy between the density distributions, ρ and δ_M, which are similar for intensity data reaching atomic resolution. The δ_M distribution at an arbitrary *r* point in the unit cell (with volume *V*) is given by the Fourier synthesis

$$\delta_M(\boldsymbol{r})=\frac{1}{V}\sum\nolimits_{\mathbf{H}}(E_{\mathbf{H}}-\langle E\rangle)e^{i\varphi_{\mathbf{H}}}e^{-i2\pi\mathbf{H}\boldsymbol{r}} \quad (1)$$

and has an associated variance (computable from the measured amplitudes) of

$$\sigma_M^2 = \frac{1}{V^2}\sum_{\mathbf{H}\neq 0}(E_{\mathbf{H}} - \langle E\rangle)^2 \qquad (2)$$

The most important difference between the δ_M distribution and ρ, the electron-density distribution with Fourier coefficients $\boldsymbol{E}_{\mathbf{H}}$ (=quasi-normalized structure factor of the **H** reflection), is some added noise in δ_M. To increase the similarity between both distributions only those δ_M peaks higher than a given threshold value are accepted. The threshold is defined in terms of the known variance, i.e. $t\cdot\sigma_M$, with $t\approx 2.5$. When refining initially random phases by δ-recycling, only the accepted δ_M peaks (up to the number of expected atoms in the unit cell) are used to calculate a new set of structure factors. The updated phases, $\varphi_{\mathbf{H}}$, are then introduced in the next δ_M Fourier synthesis to continue recycling. After a predefined number of cycles (N_{cycle}), phase refinement by δ-recycling stops and the second stage of the approach, a conventional weighted Fourier refinement, begins. The discrepancy between observed and calculated amplitudes is measured with the parameter

$$Q = 1000\cdot\left[1 - \frac{\left(\sum\sqrt{E_{\mathbf{H}}\cdot E_{c,\mathbf{H}}}\right)^2}{\sum E_{\mathbf{H}}\cdot\sum E_{c,\mathbf{H}}}\right] \qquad (3)$$

which involves in the **H** summation only the large E values [7]. Q is updated at the end of each iteration (with Q_{ini} and Q_{end} being the discrepancies at the beginning and at the end of the second stage). Trials leading to successful phase refinements are identified by low Q_{end} values. Notice that Q_{ini} is computed with the calculated $E_{c,\mathbf{H}}$ coming from the first stage and hence contains information of all reflections (strong and weak). This is in contrast to Q_{end} which results from the weighted Fourier recycling only involving the large E values (>0.7). In general, for small crystal structures and complete accurate datasets, Q_{end} for correct solutions are close to 10. Unless specifically stated, in all efficiency tests of δ-recycling 100 trials ($N_{trial}=100$) of initially-random sets of phases have been refined. The success rate (SR) measuring the efficiency of δ-recycling is the quotient between N_{sol} (=number of correct solutions) and N_{trial}.

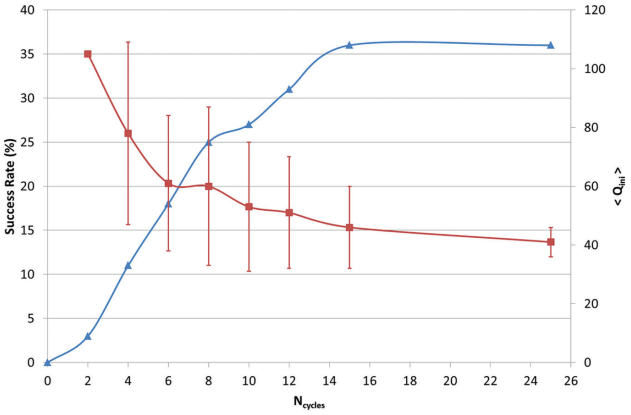

Fig. 3: Application of the δ-recycling approach to a complete dataset of calculated intensities of axinite ($N_{trial}=100$; $N_{asy}=1139$). The dependence on N_{cycle} of the success rate SR (%, triangles) and of the convergence of $\langle Q_{ini}\rangle$ (squares) with standard deviation bars is plotted. The $\langle Q_{end}\rangle$ values for correct solutions are not included because they are always 7.4(1) (irrespective of N_{cycle}).

For illustrative purposes, the evolution of δ-recycling phase refinement when applied to a complete intensity dataset of axinite is shown in Figure 3. This mineral is a triclinic complex silicate with ideal unit cell formula $Ca_4Fe^{2+}{}_2Al_4[Si_8B_2O_{30}](OH)_2$ (space group $P\bar{1}$) and unit cell dimensions $a=7.1548(5)$, $b=8.9549(7)$, $c=9.18633(6)$ Å, $\alpha=88.162(6)$, $\beta=77.345(5)$, $\gamma=81.564(7)°$, $V=568.1$ Å^3 [2]. It contains the borosilicate anion $[Si_8B_2O_{30}]^{22-}$. As shown in the figure, for $N_{cycle}=0$ (only the second stage is carried out), no solution is obtained. Up to $N_{cycle}=15$, SR steadily increases. Around $N_{cycle}\approx 15$, SR stabilizes, and convergence

Tab. 1: Success rates (SR in %) of δ-recycling as a function of the c_{acc} completeness (%) for $d_{min}=1.01$ Å ($N_{asy}=1139$) with intensities from an axinite model.

ϕ_{min}, ϕ_{max}	a				b				c			
	SR	$\langle Q_{ini}\rangle$	$\langle Q_{end}\rangle$	c_{acc}	SR	$\langle Q_{ini}\rangle$	$\langle Q_{end}\rangle$	c_{acc}	SR	$\langle Q_{ini}\rangle$	$\langle Q_{end}\rangle$	c_{acc}
−45, 45°	14	81(13)	19(3)	63	36	65(9)	15.0(3)	78	32	59.8(4)	12.2(1)	81
−40, 40°	4	91(14)	24(3)	58	18	75(12)	16(1)	72	32	67(14)	14(1)	75
−35, 35°	1	99	25	52	18	84(8)	20(2)	66	33	78(11)	17(1)	69
−30, 30°	0	–	–	47	12	94(19	22(3)	61	14	86(8)	20(3)	63
−25, 25°	–	–	–	41	8	80(10)	26(4)	53	6	94(11)	25(2)	56

Datasets obtained by simulating series of ϕ-scans with different outer ϕ limits (a) for a single χ value ($\chi=0°$; $N_{cycle}=25$–32); (b) for orthogonal χ's ($\chi=0°$ and 90°; $N_{cycle}=29$–35); (c) for χ from 0 to 360° ($N_{cycle}=30$–36).

continues down to $<Q_{ini}>=40.0(1)$ and $<Q_{end}>=7.4(1)$ for $N_{cycle}=41$. Corresponding discrepancies for wrong trials are $<Q_{ini}>_w=88(7)$ and $<Q_{end}>_w=44(3)$, so that the correct solutions can easily be discriminated.

The main requirement for the applicability of the δ-recycling approach is that the 'atomic' peaks are well resolved in the Fourier map. Since the peak shape depends on the amount and distribution of the measured intensities in the Ewald sphere, missing diffraction data can affect the efficiency of δ-recycling. For tts-μXRD the reduction of observed reflections can be due to the presence of a large background (e.g. a thick glass-substrate), to the particular experimental setup limiting the accessible portion of reciprocal space (e.g. no free rotation of the polished thin-sections) and to the diffracting volume reduction if the illuminated embedded microcrystal partially leaves the gauge volume during rotation.

Experimental

All the described tts-μXRD experiments were carried out at the microdiffraction/high pressure station of the MSPD beamline (ALBA Synchrotron) [8]. This endstation is equipped with Kirkpatrick-Baez mirrors providing a monochromatic focused beam of 15×15 μm^2 (FWHM) size and a Rayonix SX165 CCD detector (round active area of 165 mm diameter, frame size 2048×2048 pixels, 79 μm pixel size, dynamic range 16 bit). The energy used in all experiments was 29.2 keV ($\lambda=0.4246$ Å) determined from the Sn absorption K-edge. The sample-detector distance (160–185 mm) and the beam centre positions were calibrated from LaB_6 diffraction data measured at exactly the same conditions as the sample. The sample is placed in a *xyz* stage with a vertical tilt axis and visually mounted normal to the beam with the mineral in the thin-section always facing to the detector. The transparent glass-substrate allows selecting the measurement point directly with the coaxial microvisualization system (Figure 1).

Specific measurement conditions

Quartz-arenite: Sample-detector distance = 183.5 mm, minimum *d*-spacing (d_{min}) = 1.06 Å, glass-substrate thickness = 1 mm; time/frame = 4 s; $\Delta\phi=10°$, offset angles of the measured frames are ±10 and 0°.

Chladniite: Sample-detector distance = 185.15 mm, $d_{min}=1.056$ Å, glass-substrate thickness = 0.1 mm, time/frame = 5 s, $\Delta\phi=5°$, offset angles of the measured frames are ±30, ±25, ±20, ±15, ±10, ±5 and 0°.

Axinite: Sample-detector distance = 179.6 mm; $d_{min}=1.013$ Å, glass-substrate thickness = 1.1 mm, time/frame = 5 s, $\Delta\phi$ is 7.5°. Two orthogonal series of 11 ϕ-scans (at $\chi=0°$ and $\chi=90°$) were measured at one selected microvolume. Offset angles of the measured frames are ±37.5, ±30.0, ±22.5, ±15.0, ±7.5 and 0.0°. Since the outer ϕ limits are (–45, 45°), a total ϕ interval of 90° is covered.

The tts-μXRD data were processed with the TTS_software [9] consisting of the following basic units: TTS_REDUC (automated intensity extraction from 2D frames), TTS_INCO (orientation determination of the central frame of the series of ϕ-scans & orientation refinement and generation of the individual frame datasets), TTS_MERGE (frame-merging converts the frame datasets of a series into a single partial *hkl* dataset; subsequently, multicrystal merging combines the partial *hkl* datasets into the final one) and TTS_CEFREF (refinement of unit cell parameters). The manipulation of 2D frames was done with the complementary D2dplot software [10] which, among its many general utilities for 2D diffraction data processing, allows visually controlling the peak integration process and to check the orientation search results. The δ-recycling approach is implemented in the XLENS®_v1 code [11]. The supplementary material contains the diffraction images and corresponding calculations.

Comparison of data collection strategies

The phasing efficiency of the δ-recycling approach was first checked on intensities derived from an axinite model by simulating single series of ϕ-scans ranging from [$\phi_{min}=-25$, $\phi_{max}=25°$] to [–45, 45°]. [Simulation conditions: $\lambda=0.4246$ Å, sample-detector distance = 165 mm, $d_{min}=0.95$ Å, no glass-substrate]. Since axinite is triclinic, completeness is low. The results in Table 1 (part a) show that δ-recycling only works for total ϕ intervals higher than [–40, 40°] which corresponds to c_{acc} values of ~60%. It is clear that such high angular limits are difficult to attain routinely (especially for thick glass-substrates and/or if the diffracting volume of the microcrystal markedly changes during rotation), so that a data collection strategy requiring lower angular limits, i.e. maximizing the completeness per measured microvolume, is necessary.

Such a data collection strategy (hereafter, orthogonal χ strategy) results from introducing a second series of ϕ-scans with *x* (instead of *z*, Figure 1) as rotation axis, i.e. by collecting data at $\chi=90°$ [12]. In this way a large region of the Ewald sphere which was inaccessible for $\chi=0°$, can be measured (Figure 4). Table 1 (part b) shows the large c_{acc} increment when passing from the single to the orthogonal χ strategy ($\Delta c_{acc}=$ ~14%) and also the increased δ-recycling efficiency, e.g. for the rather small [–30, 30°] interval a *SR* of 12% is already found. For [–35, 35°], *SR* rises to 18% with $<Q_{ini}>$ and $<Q_{end}>$ being 84(8) and 20(2), respectively [for comparison, corresponding $<Q_{ini}>_w$ and $<Q_{end}>_w$ values are 120(14) and 53(12)]. Since [–30, 30°] and [–35, 35°] define the smallest angular limits allowing straightforward phasing, the effect of data resolution on the δ-recycling efficiency has been investigated for these two intervals, exclusively. The corresponding triplets of success rates for $d_{min}=0.95$, 1.01 and 1.08 Å resolutions are: 13, 12 and 0% for [–30, 30°]; 31, 18 and 5% for [–35, 35°] which confirms that the ideal situation for δ-recycling is for data reaching 1 Å resolution. In general, when working with ~1 mm thick glass-substrates, accurate tts data in the [–35, 35°] interval can still be acquired which means that phasing of triclinic data from a single microvolume by δ-recycling is feasible.

Completeness can be increased somewhat more, by performing multiple series of ϕ-scans at different χ values (multiple χ strategy). Simulations for this strategy are given in Table 1 (part c) wherein for simplicity a continuous χ range going from 0° to 360° has been assumed; consequently, the listed values represent the maximum attainable completeness. It can be seen that, for the triclinic case, the passage from the orthogonal to the multiple χ strategy is associated with a modest increment ($\Delta c_{acc}=$ ~3%). In practice, three series of ϕ-scans with $\Delta\chi$ increments of 0, 60 and 120° should be enough to reach the maximum completeness increment.

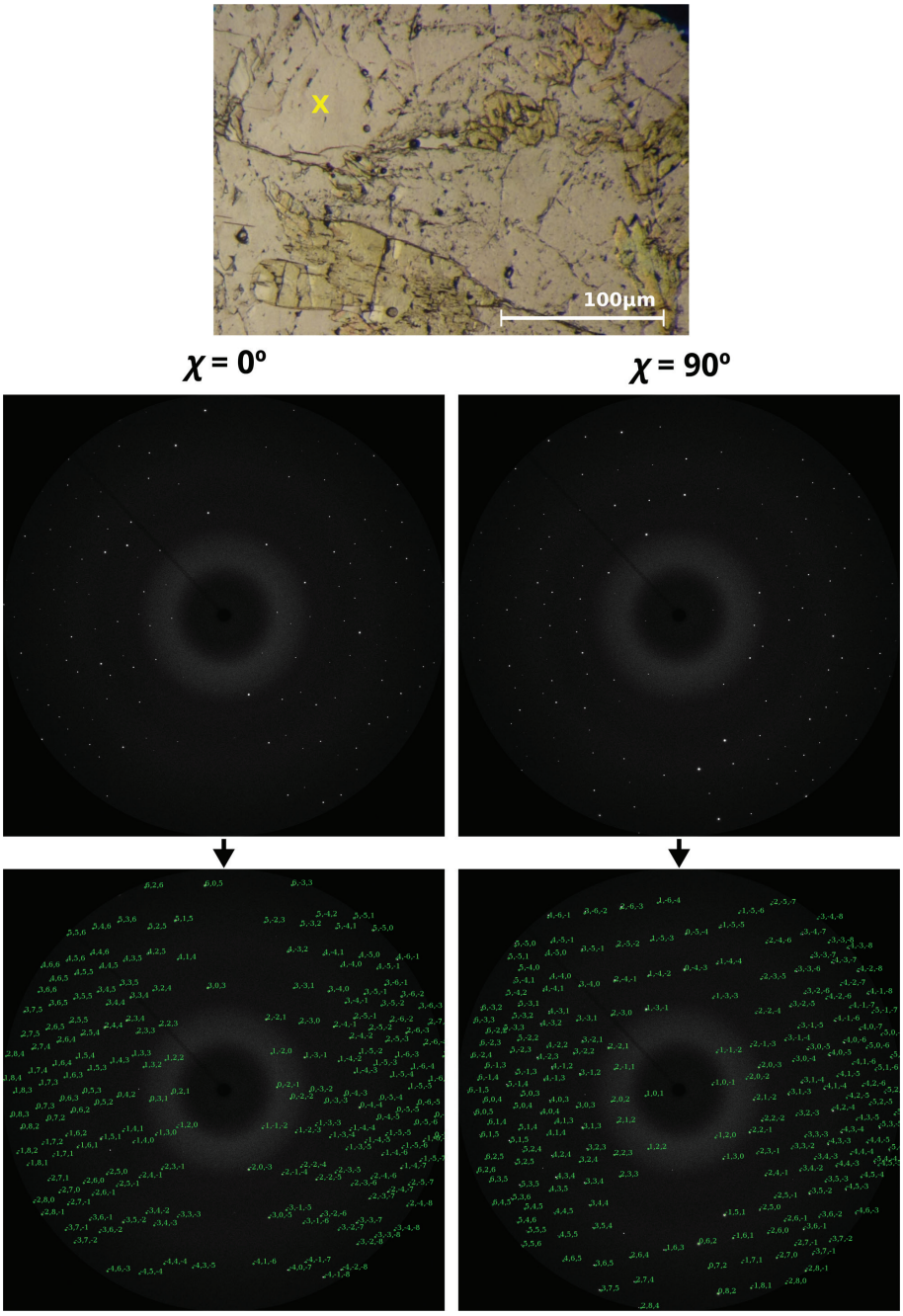

Fig. 4: Collection of two orthogonal series of ϕ-scans at one axinite microvolume (yellow cross): (left) at $\chi = 0°$ and (right) at $\chi = 90°$. The plotted frames (raw and indexed) span a ϕ rotation interval of 15°.

Results of the orthogonal χ strategy with experimental data

Axinite-(Fe): a low-symmetry case

To complement the tests with simulated data, additional ones were performed with experimental synchrotron tts data of axinite. The polished thin-section containing axinite-(Fe) corresponds to an epidote-pyroxene-axinite rock of pneumatolitic origin cropping out close to Pont de Suert (Catalonia, Spain). Two orthogonal series of 11 ϕ-scans (at $\chi = 0°$ and $\chi = 90°$) were measured at one selected microvolume (see "Experimental" Section for details). The total measured ϕ interval is 90°. Angular limits of the individual series of ϕ-scans and most relevant information related to the orthogonal χ strategy are given in

Tab. 2: Axinite-(Fe): (Left) χ values and angular limits with completeness (c_{obs} in %) for the individual series of ϕ-scans ($N_{asy}=1139$ for $d_{min}=1.01$ Å); (right) $<\phi_{max}-\phi_{min}>$ = average of ($\phi_{max}=\phi_{min}$) intervals for $\chi=0$ and 90°; R_{mult} (%) is the residual from merging the $\chi=0°$ and the $\chi=90°$ datasets and c_{obs} (%) and c_{acc} (%) the corresponding completeness values.

χ	ϕ_{min}, ϕ_{max}	c_{obs}	$<\phi_{max}-\phi_{min}>/2$	R_{mult}	c_{obs}	c_{acc}
0°	−37.5, 45.0	45	39.4	2.9	56	71
90°	−30.0, 45.0	43				
0°	−37.5, 45.0	45	37.5	2.9	54	68
90°	−22.5, 45.0	39				
0°	−37.5, 37.5	43	33.8	2.7	51	64
90°	−22.5, 37.5	36				
0°	−30.0, 37.5	40	31.9	2.5	49	61
90°	−22.5, 37.5	36				

Tab. 3: Axinite-(Fe): application of δ-recycling to triclinic data acquired with the orthogonal χ strategy showing the dependence of the success rate (*SR* in %) on the completeness (c_{obs} in %).

$<\phi_{max}-\phi_{min}>/2$	c_{obs}	*SR*	$<Q_{ini}>$	$<Q_{end}>$	N_{cycle}
39.4	56	29	70(8)	21(1)	35
37.5	54	22	72(13)	22(2)	34
33.8	51	11[a]	81(10)	27(3)	33
31.9	49	9[a]	87(10)	30(3)	32

Details on the individual series of ϕ-scans leading to $<\phi_{max}-\phi_{min}>$ are in Table 2. [a]$N_{trial}=1000$.

Table 2. The two orthogonal series were processed individually, i.e. by doing the respective frame-merging separately. Since for the second series the orientation of the thin-section plane is the same, $\Delta\chi=90°$ already specifies the crystal orientation. Finally, the two partial datasets were combined applying the multicrystal-merging procedure. Table 2 shows that completeness increases by 29(2)%, ($c_{obs}/<c_{obs*}>=1.29$), when passing from the single to the orthogonal χ strategy.

Inspection of Table 2 also indicates that the fraction of non-detected reflections is $(c_{acc}-c_{obs})/c_{acc}\approx0.2$. For the axinite-(Fe) data, the smallest detected E value is 0.16. According to the centric theoretical probability distribution of the E's [13] the approximate upper E limit for a fraction of non-detected reflections of 0.2 is approximately 0.18 which agree well with the experimental value. Since this upper limit is rather low, δ-recycling was applied by assuming zero intensities for non-detected reflections (attempts were made to introduce an expected intensity value but the corresponding phase refinement results were insensitive to it). Table 3 shows a *SR* of ~15% already for $<\phi_{max}-\phi_{min}>/2$ close to 35° which corresponds to $c_{obs}\sim52\%$. For $<\phi_{max}-\phi_{min}>/2\sim39°$ and $c_{obs}\sim56\%$, *SR* is ~30% and $<Q_{ini}>$ around 70, which are in the same order than the best ones achieved in the simulations (Table 1b and c).

Chladniite: a high-symmetry case

Due to the Laue symmetry redundancy, the degree of completeness of compounds with symmetries higher than monoclinic tends to be high, so that a single series of ϕ-scans normally suffices for phasing with δ-recycling. If the series of ϕ-scans is incomplete, then the orthogonal χ strategy also helps to increase the completeness. Incomplete series occur when the diffracting microcrystal partially (or completely) leaves the gauge volume during the thin-section rotation. Probable causes (neglecting eventual target positioning errors) are microcrystals only slightly larger than the beam spot, or also the uncertain evolution of the microcrystal shape with depth, e.g. the case of anhedral microcrystals forming thin veinlets within other materials. To show the viability of tts-μXRD in the latter situations, experimental tts data of an anhedral microcrystal of chladniite (chlad4) included in beusite were analyzed (Figure 5). Chladniite is a complex phosphate belonging to the fillowite group [14] which had only been found in meteorites [15]. Its chemical composition (analysed with electron microprobe and normalized to 108 P atoms) is $Na_{35.1}Ca_{16.8}Mg_{52.8}Fe_{45}Mn_{42.6}P_{108}O_{432}$. Its unit cell parameters are $a=15.0133(3)$, $c=42.887(2)$ Å, $Z=3$ with space group $R\bar{3}$ (148). Inspection of Figure 6

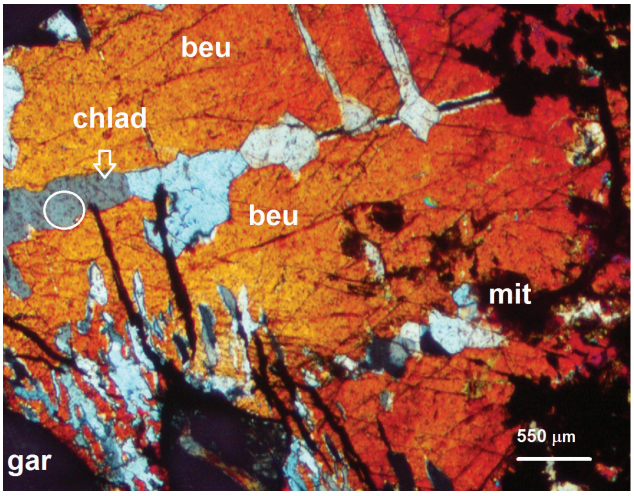

Fig. 5: Cross-polarized photomicrograph of a polished thin-section containing garnet (gar) and the three phosphates chladniite (chlad), beusite (beu) and mitridadite (mit). The chladniite microcrystals are embedded in beusite. The measurement point is inside the white circle with the ϕ rotation axis being horizontal.

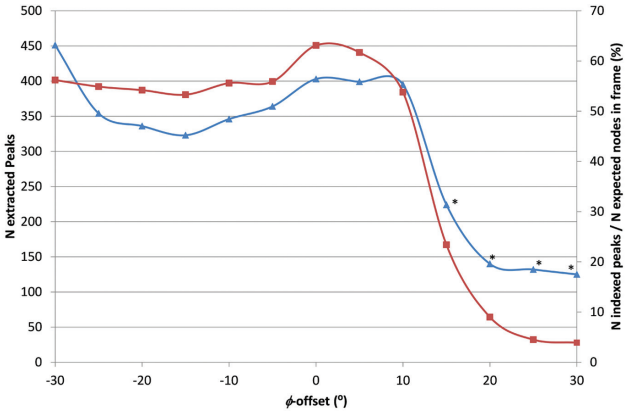

Fig. 6: Chladniite (chlad4 microvolume): a. (triangles) number of extracted peaks in each 2D frame as a function of the offset angle (°); b. (squares) percentage of indexed peaks relative to the theoretical number of nodes in the frame in terms of the offset angle (°). Frame-merging scaling factors for offset angles −30 to 5° are 0.81, 1.10, 1.15, 1.18, 0.99, 0.98, 0.87, 0.85. Points in the figure marked with *correspond to beusite gradually penetrating the gauge volume.

Tab. 4: Chladniite: application of δ-recycling to tts data derived from an incomplete series of φ-scans for two angular ranges of 45 and 35° (d_{min} = 1.043 Å; N_{asy} = 1676; respective N_{cycles} are 79 and 120).

ϕ_{min}, ϕ_{max}	*SR* (%)	$<Q_{ini}>$	$<Q_{ini}>_w$	$<Q_{end}>$	c_{obs} (%)	c_{acc} (%)
−35, 10°	40	77(6)	152(11)	19(1)	55	85
−25, 10°	19	97(7)	156(11)	30(2)	49	77

$<Q_{ini}>_w$ is the value of Q_{ini} averaged over the wrong solutions.

indicates that the number of indexed peaks decreases very fast for frames above $\phi = 10°$ due to the gradual penetration of beusite in the gauge volume. Consequently, the upper frames are not included in frame-merging (resulting $R_{frame} = 2.5\%$). The efficiency of δ-recycling for two different angular ranges is given in Table 4. Whereas for $c_{obs} = 49\%$ it amounts 19%, for $c_{obs} = 55\%$ it is much higher (40%), so that in this example, in spite of its incompleteness, a single series is enough for structure solution.

Conclusions

Thanks to its increased completeness (~29% for the triclinic case) the orthogonal χ strategy considerably reduces the total angular range of the φ-scans needed for generating intensity datasets suitable for δ-recycling phase refinement. Also for the triclinic symmetry, the minimum total range of 90° required by a single series of φ-scans reduces to 70° for the orthogonal strategy. This means that a φ rotation of only ±35° which is mostly attainable even with thick glass-substrates, is enough for solving crystal structures from data of a single microvolume. If the maximum attainable completeness is needed, a multiple χ strategy is proposed consisting of three series of φ-scans with $\Delta\chi = 0$, 60 and 120°. In contrast, for high-symmetry compounds, due to the Laue symmetry redundancy much smaller total angular ranges are tolerated, so that a single series of φ-scans normally suffices for phasing. If not, the availability of the orthogonal series of scans ensures solution from a unique target point. Needless to say, that optimizing data acquisition from a single microvolume is also beneficial for crystal structure refinement, since eventual chemical inhomogeneity is minimized.

In general, when working with mineralogical samples, a minimum c_{obs} of 0.50–0.55 is needed for getting at least ~10% successful runs with the δ-recycling approach. From a practical point of view it is best to use partially polished thin-sections on thinner glass-substrates, e.g. on common cover glasses of only 0.1 mm thickness [15]. Although the diffraction by the mineral grain is not affected (it faces the detector surface), substrate thinning significantly reduces the glass contribution to background.

Finally, it is worth mentioning that the results of this study can also be potentially useful in structure solution of crystalline phases on other substrates or when the sample rotation is partially hindered, e.g. in high-pressure diamond anvil cells where the microcrystals are confined between the diamonds.

Acknowledgements: The financial support of the Spanish 'Ministerio de Economía, Industria y Competitividad' (Projects MAT2015-67593-P and "Severo Ochoa" SEV-2015-0496) is gratefully acknowledged. Thank are also due to the ALBA synchrotron (Barcelona, Spain) for beamtime (experiment Nr. 2016021655). OV also thanks the in-house project IH15-BL04.

References

[1] J. Rius, A. Labrador, A. Crespi, C. Frontera, O. Vallcorba, J. C. Melgarejo, Capabilities of through-the-substrate microdiffraction: application of Patterson-function direct methods to synchrotron data from polished thin sections. *J. Synchrotron Rad.* **2011**, *18*, 891.

[2] J. Rius, O. Vallcorba, C. Frontera, I. Peral, A. Crespi, C. Miravitlles, Application of synchrotron through-the-substrate microdiffraction to crystals in polished thin sections. *IUCrJ* **2015**, *2*, 452.

[3] J. Rius, Direct phasing from Patterson syntheses by δ recycling. *Acta Cryst. A* **2012**, *68*, 77.

[4] J. Rius, Patterson function and δ recycling: derivation of the phasing equations. *Acta Crystallogr. A* **2012**, *68*, 399.

[5] G. Oszlány, A. Sütó, Ab initio structure solution by charge flipping. *Acta Crystallogr. A* **2004**, *60*, 134.
[6] L. Palatinus, The charge-flipping algorithm in crystallography. *Acta Crystallogr. B* **2013**, *69*, 1.
[7] J. Rius, Application of Patterson-function direct methods to materials characterisation. *IUCrJ* **2014**, *1*, 291.
[8] F. Fauth, I. Peral, C. Popescu, M. Knapp, The new materials science powder diffraction beamline at ALBA synchrotron. *Powder Diffr.* **2013**, *28*, S360.
[9] J. Rius, O. Vallcorba, C. Frontera, *TTS_software: A computer software for crystal structure analysis from tts microdiffraction data*. Institut de Ciència de Materials de Barcelona, CSIC, (Spain) **2016**. Available at departments.icmab.es/crystallogra phy/software.
[10] O. Vallcorba, J. Rius, *D2dplot: Plotting of 2D diffraction data, basic processing and phase ID*. ALBA Synchrotron Light Source – CELLS, (Spain) **2017**. Available at https://www.cells.es/en/beamlines/bl04-mspd/preparing-your-experiment.
[11] J. Rius, *XLENS®: A direct methods program for solving crystal structures single-crystal data by δ recycling*. Institut de Ciència de Materials de Barcelona, CSIC (Spain) **2013**. Available at departments.icmab.es/crystallography/software.
[12] J. R. Helliwell, Single-crystal X-ray techniques. In *International Tables for Crystallography Vol. C*. Mathematical, physical and chemical tables, (Eds. E. Prince and T. R. Welberry) Springer, Netherlands, pp. 26–41, **2006**.
[13] J. C. Wilson, The probability distribution of X-ray intensities. *Acta Crystallogr.* **1949**, *2*, 318.
[14] T. Araki, P. B. Moore, Fillowite, $Na_2Ca(Mn,Fe)_7^{2+}(PO_4)_6$: its crystal structure. *Am. Mineral.* **1981**, *66*, 827.
[15] O. Vallcorba, L. Casas, F. Colombo, C. Frontera, J. Rius, First terrestrial occurrence of the complex phosphate chladniite: Crystal-structure refinement by synchrotron through-the-substrate microdiffraction. *Eur J Mineral* **2017**, *29*, 287.

Supplemental Material: The online version of this article (DOI: 10.1515/zkri-2017-2064) offers supplementary material, available to authorized users.

Graphical Synopsis

Jordi Rius, Oriol Vallcorba, Anna Crespi and Fernando Colombo

Increasing data completeness in synchrotron tts-microdiffraction experiments for δ-recycling phasing of low-symmetry compounds

DOI 10.1515/zkri-2017-2064
Z. Kristallogr. 2017; x(x): xxx–xxx

Synopsis: Data completeness in synchrotron tts-μXRD improves with the orthogonal χ strategy which merges the information of two series of orthogonal ϕ-scans collected at the same μvolume of the polished thin section. How this extended dataset affects the efficiency of δ-recycling phasing is analyzed.